

3-1-2017

Virtual Resonant Emission and Oscillatory Long-Range Tails in Van Der Waals Interactions of Excited States: QED Treatment and Applications

Ulrich D. Jentschura

Missouri University of Science and Technology, ulj@mst.edu

Chandra Mani Adhikari

Vincent Debierre

Follow this and additional works at: http://scholarsmine.mst.edu/phys_facwork



Part of the [Physics Commons](#)

Recommended Citation

U. D. Jentschura et al., "Virtual Resonant Emission and Oscillatory Long-Range Tails in Van Der Waals Interactions of Excited States: QED Treatment and Applications," *Physical Review Letters*, vol. 118, no. 12, pp. 123001-1-123001-6, American Physical Society (APS), Mar 2017.

The definitive version is available at <http://dx.doi.org/10.1103/PhysRevLett.118.123001>

This Article - Journal is brought to you for free and open access by Scholars' Mine. It has been accepted for inclusion in Physics Faculty Research & Creative Works by an authorized administrator of Scholars' Mine. This work is protected by U. S. Copyright Law. Unauthorized use including reproduction for redistribution requires the permission of the copyright holder. For more information, please contact scholarsmine@mst.edu.

Virtual Resonant Emission and Oscillatory Long-Range Tails in van der Waals Interactions of Excited States: QED Treatment and Applications

U. D. Jentschura, C. M. Adhikari, and V. Debierre

Department of Physics, Missouri University of Science and Technology, Rolla, Missouri 65409, USA

(Received 12 September 2016; revised manuscript received 15 February 2017; published 20 March 2017)

We report on a quantum electrodynamic (QED) investigation of the interaction between a ground state atom with another atom in an excited state. General expressions, applicable to any atom, are indicated for the long-range tails that are due to virtual resonant emission and absorption into and from vacuum modes whose frequency equals the transition frequency to available lower-lying atomic states. For identical atoms, one of which is in an excited state, we also discuss the mixing term that depends on the symmetry of the two-atom wave function (these evolve into either the gerade or the ungerade state for close approach), and we include all nonresonant states in our rigorous QED treatment. In order to illustrate the findings, we analyze the fine-structure resolved van der Waals interaction for nD - $1S$ hydrogen interactions with $n = 8, 10, 12$ and find surprisingly large numerical coefficients.

DOI: 10.1103/PhysRevLett.118.123001

Introduction.—While the long-range interaction between two ground state atoms has been fully understood in all interatomic separation regimes since the work of Casimir and Polder [1], a completely new situation arises when one of the atoms is in an excited state [2–7]. In particular, several recent studies [8–12] have reported on long-range, space-wise-oscillating tails, which decay as slowly as R^{-2} (R is the interatomic separation). For excited reference states, these tails parametrically dominate over the usual Casimir-Polder type R^{-7} interaction [1]. Conflicting results have been obtained for the oscillating tails [6,7,13]. One important question concerns the ratio of the oscillatory, resonant terms to the nonoscillatory, nonresonant contributions to van der Waals interactions, and the matching and interpolation of the results with the familiar close-range, nonretarded van der Waals limit of the interatomic interaction. Our aim here is to advance the theory of excited-state interatomic interactions, by including the nonresonant states, the dynamically induced correction to the atomic decay width (distance-dependent imaginary part of the energy shift), and the additional terms that occur for identical atoms (namely, the gerade-ungerade mixing term [2]).

As an example application, we study a system where a highly excited D state interacts with a ground state ($1S$) hydrogen atom (see Refs. [14–16]). In this system, the availability of low-energy P and F states for virtual dipole transitions from the nD state makes the oscillating long-range tails relevant. An improved understanding is necessary for the interpretation of experiments involving general Rydberg states [17], in regard to the determination of fundamental constants. We concentrate on nD - $1S$ interactions with $n = 8, 10, 12$. The projection- and symmetry-averaged C_6 van der Waals coefficient of the $12D$ - $1S$ system amounts to a surprisingly large numerical value

$\langle C_6(12D; 1S) \rangle = 227756$ in atomic units. SI mksA units are used throughout this Letter.

Formalism.—The general idea behind the matching of the scattering amplitude and the effective Hamiltonian has been described in Chap. 85 of Ref. [18], in the context of the interatomic interaction. In short, one uses the relation

$$\langle \psi'_A, \psi'_B | U(\vec{r}_A, \vec{r}_B, \vec{R}) | \psi_A, \psi_B \rangle = \frac{i\hbar}{T} S_{A'B'AB}, \quad (1)$$

where $|\psi_A, \psi_B\rangle$ is the initial state of the two-atom system, $|\psi'_A, \psi'_B\rangle$ is the final state, and $H_{\text{eff}} = U(\vec{r}_A, \vec{r}_B, \vec{R})$ is the effective potential that depends on the electron coordinates \vec{r}_i (where $i = A, B$ denotes the atom). The interatomic distance vector is \vec{R} . Finally, T is the long time interval that results from the integration over the interaction in the S matrix formalism [see Eq. (85.2) of Ref. [18]].

It becomes necessary to generalize the treatment outlined in Eqs. (85.1)–(85.14) of Ref. [18] to the case of identical atoms, one of which is in an excited state. In this case, one has to treat a mixing term [2], which describes a scattering process in which the state $|\psi_A, \psi_B\rangle$ is scattered into the state $|\psi_B, \psi_A\rangle$; the two atoms in this case “interchange” their quantum states. The eigenstates of the van der Waals Hamiltonian [2] are states of the form $(1/\sqrt{2})(|\psi_A, \psi_B\rangle \pm |\psi_B, \psi_A\rangle)$, and the interaction energy ΔE is the sum of a direct term (which is contained in the canonical derivations, e.g., Ref. [18]), and a mixing term, which is added here and whose sign depends on the symmetry of the two-atom state (\pm). We find the following general expression (further details can be found in the Supplemental Material, Ref. [19]), including retardation, for the electrodynamic interaction between two atoms A and B in arbitrary states,

$$\Delta E = \frac{i}{\hbar} \int_0^\infty \frac{d\omega}{2\pi} \omega^4 D_{ij}(\omega, \vec{R}) D_{k\ell}(\omega, \vec{R}) \times [\alpha_{A,ik}(\omega) \alpha_{B,j\ell}(\omega) \pm \alpha_{\underline{AB},ik}(\omega) \alpha_{\underline{AB},j\ell}(\omega)], \quad (2)$$

where the last term describes the mixing and is present only for identical atoms. The photon propagator (in the temporal gauge) and the tensor polarizabilities are given by

$$D_{ij}(\omega, \vec{R}) = \frac{\hbar}{4\pi\epsilon_0 c^2} [\alpha_{ij} + \beta_{ij} f(\omega, R)] \frac{e^{i(\sqrt{\omega^2 + ie/c} R)}{R}, \quad (3a)$$

$$\alpha_{A,ij}(\omega) = \sum_v \left(\frac{\langle \psi_A | d_{Ai} | v_A \rangle \langle v_A | d_{Aj} | \psi_A \rangle}{E_{v,A} - \hbar\omega - i\epsilon} + \frac{\langle \psi_A | d_{Ai} | v_A \rangle \langle v_A | d_{Aj} | \psi_A \rangle}{E_{v,A} + \hbar\omega - i\epsilon} \right), \quad (3b)$$

$$\alpha_{\underline{AB},ij}(\omega) = \sum_v \left(\frac{\langle \psi_A | d_{Ai} | v_A \rangle \langle v_B | d_{Bj} | \psi_B \rangle}{E_{v,A} - \hbar\omega - i\epsilon} + \frac{\langle \psi_A | d_{Ai} | v_A \rangle \langle v_B | d_{Bj} | \psi_B \rangle}{E_{v,A} + \hbar\omega - i\epsilon} \right). \quad (3c)$$

Here, $f(\omega, R) = ic/|\omega R - c^2/\omega^2 R^2$, and the tensor structures are $\alpha_{ij} = \delta_{ij} - R_i R_j / R^2$ and $\beta_{ij} = \delta_{ij} - 3(R_i R_j / R^2)$. The speed of light is c , and ϵ_0 is the vacuum permittivity. The (excited) state of atom A is $|\psi_A\rangle$, and \vec{d}_A is the electric dipole operator for the same atom. We also write $E_{v,A} \equiv E_v - E_A$ and $E_{v,B} \equiv E_v - E_B$. As usual, the dipole polarizability is given by a sum over all virtual states of atom A that are accessible from $|\psi_A\rangle$ through an electric dipole transition. The tensor polarizability $\alpha_{\underline{AB},ij}(\omega)$ is obtained from $\alpha_{\underline{AB},ij}(\omega)$ by a replacement $E_{v,A} \rightarrow E_{v,B}$ in the propagator denominators. For excited reference states, it is crucial that the polarizabilities (3b) and (3c) have the poles placed according to the Feynman prescription; this follows from the time-ordered dipole operators which naturally occur in time-ordered products of the interaction Hamiltonian in the S matrix.

If atom A is in an excited state and B in the ground state, then the interaction energy $\Delta E = \mathcal{Q} + \mathcal{W}$ [see Eq. (2)] can be split into a Wick-rotated term ($\omega \rightarrow i\omega$)

$$\mathcal{W} = -\frac{1}{\hbar} \int_0^\infty \frac{d\omega}{2\pi} \omega^4 D_{ij}(i\omega, \vec{R}) D_{k\ell}(i\omega, \vec{R}) \times [\alpha_{A,ik}(i\omega) \alpha_{B,j\ell}(i\omega) \pm \alpha_{\underline{AB},ik}(i\omega) \alpha_{\underline{AB},j\ell}(i\omega)], \quad (4)$$

and a pole term from the residues at $\omega = -E_{m,A}/\hbar + i\epsilon$,

$$\mathcal{Q} = \sum_{E_{m,A} < 0} \frac{\langle \psi_A | d_{Ai} | m_A \rangle}{(4\pi\epsilon_0)^2 R^6} \left[\langle m_A | d_{Ak} | \psi_A \rangle \alpha_{B,j\ell} \left(\frac{E_{m,A}}{\hbar} \right) \pm \langle m_A | d_{Bk} | \psi_B \rangle \alpha_{\underline{AB},j\ell} \left(\frac{E_{m,A}}{\hbar} \right) \right] f_{ijk\ell}(r_{m,A}), \quad (5a)$$

$$f_{ijk\ell}(r) = -\exp(-2ir) [\beta_{ij} \beta_{k\ell} (1 + 2ir) - (2\alpha_{ij} \beta_{k\ell} + \beta_{ij} \beta_{k\ell}) r^2 - 2i\alpha_{ij} \beta_{k\ell} r^3 + \alpha_{ij} \alpha_{k\ell} r^4], \quad (5b)$$

$$\text{Re} f_{ijk\ell}(r) = -\cos(2r) [\beta_{ij} \beta_{k\ell} - (2\alpha_{ij} \beta_{k\ell} + \beta_{ij} \beta_{k\ell}) r^2 + \alpha_{ij} \alpha_{k\ell} r^4] - 2r \sin(r) [\beta_{ij} \beta_{k\ell} - \alpha_{ij} \beta_{k\ell} r^2], \quad (5c)$$

$$\text{Im} f_{ijk\ell}(r) = -\frac{1}{2} \{ -2 \sin(2r) [\beta_{ij} \beta_{k\ell} - (2\alpha_{ij} \beta_{k\ell} + \beta_{ij} \beta_{k\ell}) r^2 + \alpha_{ij} \alpha_{k\ell} r^4] + 4r \cos(r) [\beta_{ij} \beta_{k\ell} - \alpha_{ij} \beta_{k\ell} r^2] \}, \quad (5d)$$

where

$$r_{m,A} = \frac{E_{m,A} R}{\hbar c}, \quad E_{m,A} \equiv E_{m_A} - E_A. \quad (6)$$

Here, the sum is taken over all states m that are accessible from $|\psi_A\rangle$ by a dipole transition *and* of lower energy than $|\psi_A\rangle$. For a general atom, the generalization is trivial: one simply sums the dipole operators of atom A over the electrons.

The pole term induces both a real, oscillatory, distance-dependent energy shift as well as a correction to the width of the excited state,

$$\mathcal{Q} = \mathcal{P} - \frac{i}{2} \Gamma, \quad (7)$$

where Γ is obtained from Eq. (5a) by substituting for $f_{ijk\ell}(r)$ the expression in curly brackets in Eq. (5d).

From a QED point of view, the real part of the energy shift corresponding to the pole term is due to a very peculiar process, namely, resonant virtual emission into vacuum modes whose angular frequency matches the resonance condition $\omega = -E_{m,A} = |E_{m,A}|$. The resonant emission is accompanied by resonant absorption, and therefore leads to a real, rather than imaginary, energy shift. In the ladder and crossed-ladder Feynman diagrams (see Fig. 1), the virtual electron line of atom A , in state $|\psi_A\rangle$, would turn into a resonant lower-lying virtual state, whereas the ground-state atom line is excited into a “normal” energetically higher virtual state $|v_B\rangle$. The imaginary part of the pole term describes a process where the virtual photon becomes real

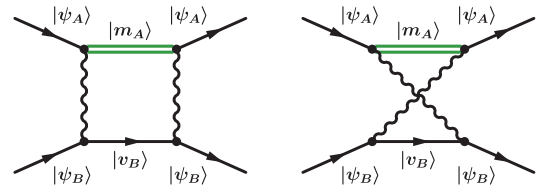


FIG. 1. Ladder and crossed-ladder Feynman diagrams for the long-range interaction of atoms. The virtual state of atom A , labeled $|m_A\rangle$, is assumed to have a lower energy than the reference state.

and is emitted by the atom, in analogy to the imaginary part of the self energy [20,21]. Feynman propagators allow us to reduce the calculation to only two Feynman diagrams, which capture all possible time orderings (in contrast to time-ordered perturbation theory).

In Ref. [11], a situation of two nonidentical atoms is considered, with mutually close resonance energies $\hbar\omega_A$ and $\hbar\omega_B$. Setting $E_{m,A} = -\hbar\omega_A$ and $E_{q,B} = \hbar\omega_B$, the authors of Ref. [11] assume that $\omega_A \approx \omega_B$, and define $\Delta_{AB} = \hbar\omega_A - \hbar\omega_B$ with $|\Delta_{AB}| \ll \hbar\omega_A, \hbar\omega_B$. Furthermore, they restrict the sum over virtual states in Eq. (5) to the resonant state only, and they only keep the term $1/(E_{m,A} + E_{q,B})$ in the sum over virtual states, in the polarizability $\alpha_B(E_{m,A}/\hbar)$ [see Eq. (5)]. Under their assumptions [see Eq. (4) of Ref. [11]], $|1/(E_{m,A} + E_{q,B})| = |-1/\Delta_{AB}| \gg |1/(E_{q,B} - E_{m,A})| \approx 1/(2\hbar\omega_B)$.

Under the restriction to the resonant virtual states, the direct term in Eq. (5) [proportional to $\alpha_{B,j\ell}(E_{m,A}/\hbar)$] matches that reported in Ref. [11] if we average the latter over the interaction time $T > 2R/c$. Our result adds the contribution from nonresonant virtual states, which allow us to match the result with the close-range (van der Waals) limit, as well as the mixing term [proportional to $\alpha_{AB,j\ell}(E_{m,A}/\hbar)$] and the imaginary part of the energy shift (width term). For the mixing term to be nonzero, we need the orbital angular momentum quantum numbers to fulfill the relation $\ell_A = \ell_B$ or $|\ell_A - \ell_B| = 2$, by virtue of the usual selection rules of atomic physics. Furthermore, we find that the full consideration of the Wick-rotated term and the pole term is crucial for obtaining numerically correct results for the interaction energies, for surprisingly large interatomic distances.

Numerical calculations.—In the following, we aim to apply the developed formalism to $nD-1S$ atomic hydrogen systems. The interaction energy depends both on the spin orientation of the electron (total angular momentum J) as well as its projection μ onto the quantization axis [19]. One may eliminate this dependence by evaluating the average over the fine-structure resolved states.

Short range.—For interatomic separations in the range $a_0 \ll R \ll a_0/\alpha$ (where a_0 is the Bohr radius), the interaction energy (2) is well approximated as $\Delta E \approx \Delta E_{\text{vdW}}$, where

$$\begin{aligned} \Delta E_{\text{vdW}} &= -\frac{1}{(4\pi\epsilon_0)^2} \frac{\beta_{ij}\beta_{k\ell}}{R^6} \sum_v \sum_q \frac{1}{E_{v,A} + E_{q,B}} \\ &\times [\langle \psi_A | d_{Ai} | v_A \rangle \langle v_A | d_{Ak} | \psi_A \rangle \langle \psi_B | d_{Bj} | q_B \rangle \\ &\times \langle q_B | d_{B\ell} | \psi_B \rangle \pm \langle \psi_A | d_{Ai} | v_A \rangle \langle v_B | d_{Bk} | \psi_B \rangle \\ &\times \langle \psi_B | d_{Bj} | q_B \rangle \langle q_A | d_{A\ell} | \psi_A \rangle], \\ &= -\frac{1}{R^6} [D_6(A; B) \pm M_6(A; B)]. \end{aligned} \quad (8)$$

Here, D_6 is the direct, and M_6 is the mixing van der Waals coefficient [2–7]. For energetically lower states in atom A (with $E_{v,A} = E_{m,A} < 0$), the representation (8) is obtained by

TABLE I. van der Waals D_6 (direct) coefficients, for $nD-1S$ interactions, averaged over the total angular momenta and magnetic projections of the excited D state. The coefficients are given in units of $E_h a_0^6$.

Coefficient	Virtual P	Virtual F	Total
$\langle D_6(8D; 1S) \rangle$	17 459.439	26 156.866	43 616.296
$\langle D_6(10D; 1S) \rangle$	43 476.563	65 182.580	108 659.144
$\langle D_6(12D; 1S) \rangle$	91 115.328	136 640.733	227 756.061

carefully considering the contributions from the Wick-rotated term \mathcal{W} and the pole term \mathcal{P} .

For the fine-structure average of the direct term D_6 , we have

$$\langle D_6(nD; 1S) \rangle = \langle D_6^{(P)}(nD; 1S) \rangle + \langle D_6^{(F)}(nD; 1S) \rangle, \quad (9)$$

where the virtual- P -state contribution $\langle D_6^{(P)}(nD; 1S) \rangle$ and the virtual- F -state contribution $\langle D_6^{(F)}(nD; 1S) \rangle$ are given in Table I. Numerically, we find that the mixing term M_6 is smaller than the direct term D_6 , by at least 4 orders of magnitude, for all fine-structure resolved nD states, for all distance ranges investigated in this Letter. This trend follows the pattern observed for the van der Waals coefficients (Table I) and is in contrast to the $2S-1S$ system, where both terms are of comparable magnitude [2,4].

Long range.—One might think that the $1/R^2$ pole term from Eq. (5) should easily dominate the interaction energy in the range $R \gg a_0/\alpha$. Indeed, power counting in the fine-structure constant α , according to Ref. [22], shows that the cosine and sine terms in \mathcal{P} are asymptotically given by

$$\frac{\mathcal{P}_{\text{cos}}}{E_h} \sim \left\{ \frac{\alpha^4}{\rho^2} \cos(\alpha\rho), \frac{\alpha^2}{\rho^4} \cos(\alpha\rho), \frac{1}{\rho^6} \cos(\alpha\rho) \right\}, \quad (10a)$$

$$\frac{\mathcal{P}_{\text{sin}}}{E_h} \sim \left\{ \frac{\alpha^3}{\rho^3} \sin(\alpha\rho), \frac{\alpha}{\rho^5} \sin(\alpha\rho) \right\}, \quad (10b)$$

where $\rho = R/a_0$ and E_h is the Hartree energy. A comparison to the van der Waals term, given in Eq. (8), and the Wick-rotated term (4),

$$\Delta E_{\text{vdW}} \sim \frac{E_h}{\rho^6}, \quad \mathcal{W} \stackrel{\rho \gg 1/\alpha}{\sim} \frac{E_h}{\alpha\rho^7}, \quad (10c)$$

shows that all terms (pole term, Wick-rotated, and van der Waals) are of the same order of magnitude for $\rho \sim 1/\alpha$, while the pole term should parametrically dominate for $\rho > 1/\alpha$. However, this consideration does not take into account the scaling of the terms with the principal quantum number n . While we find that the D_6 coefficients typically grow as n^4 for a given manifold of states (see also Ref. [23]), the energy differences $E_{m,A}$ for adjacent lower-lying states are

proportional to $1/(n-1)^2 - 1/n^2 \sim 1/n^3$ for large n , and the fourth power of the energy difference $E_{m,A}$ enters the prefactor of the $1/R^2$ pole term. Hence, it is interesting to compare the parametric estimates to a concrete calculation for excited nD states; this is also important in order to gauge the importance of the nonresonant contributions to the interaction energy which were left out in Ref. [11].

But let us first write down the leading asymptotic terms, for all long-range contributions of interest. For $R \gg \hbar c/\mathcal{L}$, where \mathcal{L} is the Lamb shift energy of about 1 GHz (see Ref. [4]), the Wick-rotated contribution attains the familiar $1/R^7$ asymptotics from the Casimir-Polder formalism [1],

$$\mathcal{W}^{(\text{dir})} \stackrel{R \rightarrow \infty}{\equiv} -\frac{\hbar c \alpha_{nD,ij}(0) \alpha_{1S}(0)}{8\pi (4\pi\epsilon_0)^2 R^7} \left(13\delta_{ij} + 15\frac{R_i R_j}{R^2} \right). \quad (11)$$

This tail is parametrically suppressed in comparison to the leading $1/R^2$ pole contribution,

$$\mathcal{P}^{(\text{dir})} \stackrel{R \rightarrow \infty}{\equiv} -\sum_{E_m < E_{nD}} \left(\frac{E_{m,A}}{\hbar c} \right)^4 \frac{\cos\left(2\frac{E_{m,A}}{\hbar c} R\right)}{(4\pi\epsilon_0)^2 R^2} \times \alpha_{ij} \langle nD | d_{Ai} | m_A \rangle \langle m_A | d_{Aj} | nD \rangle \alpha_{1S} \left(\frac{E_{m,A}}{\hbar} \right). \quad (12)$$

In the intermediate range $a_0 \ll R \ll \hbar c/\mathcal{L}$, the Wick-rotated contribution has a nonretarded $1/R^6$ tail, due to a nonretarded contribution from virtual nP and nF states, which are displaced from the nD state only by the Lamb shift [see Eqs. (23) and (24) of Ref. [4]],

$$\mathcal{W}^{(\text{dir})} \sim -\frac{\bar{D}_6(nD; 1S)}{R^6}, \quad \frac{a_0}{\alpha} \ll R \ll \frac{\hbar c}{\mathcal{L}}. \quad (13)$$

The fine-structure average of $\bar{D}_6(nD; 1S)$ is given by [19]

$$\langle \bar{D}_6(nD; 1S) \rangle = \frac{81}{8} n^2 (n^2 - 7). \quad (14)$$

For the mixing term, simplifications are scarce; the leading long-range asymptotics of the Wick-rotated term read

$$\mathcal{W}^{(\text{mix})} \stackrel{R \rightarrow \infty}{\equiv} -\frac{\hbar c \alpha_{nD1S,ik}(0) \alpha_{nD1S,j\ell}(0)}{8\pi (4\pi\epsilon_0)^2 R^7} \times (3\alpha_{ij}\alpha_{kl} + 5\alpha_{ij}\beta_{kl} + 5\beta_{ij}\beta_{kl}). \quad (15)$$

The leading pole contribution (in the long range) is given by a sum over virtual P states that enter the mixed polarizability $\alpha_{nD1S,j\ell}$,

$$\mathcal{P}^{(\text{mix})} \stackrel{R \rightarrow \infty}{\equiv} -\frac{\sum_{E_m < E_{nD}} \left(\frac{E_{m,A}}{\hbar c} \right)^4 \cos\left(2\frac{E_{m,A}}{\hbar c} R\right)}{(4\pi\epsilon_0)^2 R^2} \times \alpha_{ij}\alpha_{kl}\alpha_{nD1S,j\ell} \left(\frac{E_{m,A}}{\hbar} \right) \langle nD | d_{Ai} | m_A \rangle \langle m_A | d_{Ak} | 1S \rangle. \quad (16)$$

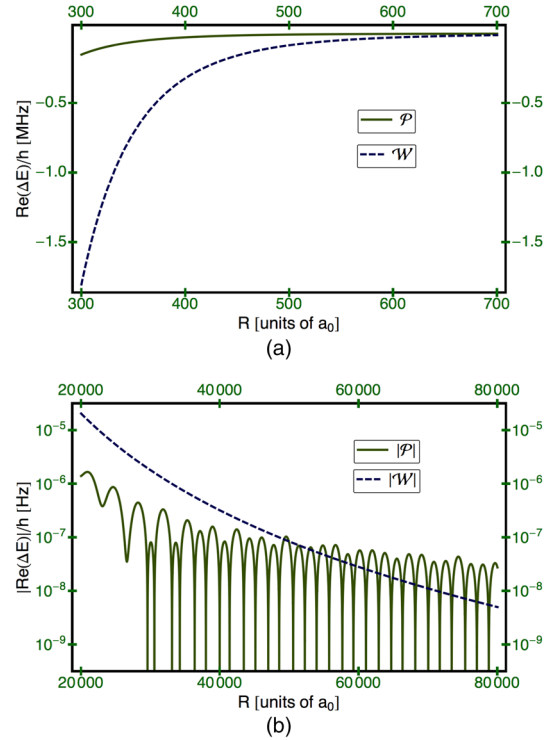


FIG. 2. The upper panel (a) compares the Wick-rotated term \mathcal{W} (dashed line) to the real part $\mathcal{P} = \text{Re}Q$ of the pole term (solid line) for the $12D-1S$ interaction (fine-structure average) in the intermediate range $a_0/\alpha \lesssim R \ll \hbar c/\mathcal{L}$. The interaction energy is $\Delta E = Q + \mathcal{W}$. The Wick-rotated term dominates despite parametric suppression [see Eq. (10)]. The lower panel (b) displays the logarithm of the modulus of the interaction energy (Wick-rotated term versus pole term) for very large interatomic distance; the pole term finally dominates. The oscillations of the pole term are dominated by virtual $2P$ state contribution; when the interaction energy changes sign, the logarithm diverges to $-\infty$.

In the intermediate range, one has

$$\mathcal{W}^{(\text{mix})} \sim -\frac{\bar{M}_6(nD; 1S)}{R^6}, \quad \frac{a_0}{\alpha} \ll R \ll \frac{\hbar c}{\mathcal{L}}, \quad (17)$$

where $\bar{M}_6(nD; 1S)$ is the generalization of \bar{D}_6 to the mixing term [see Ref. [19] and Eq. (67) of Ref. [4]].

In Fig. 2, we compare the magnitude of the Wick-rotated term and the pole term in the intermediate range $a_0/\alpha \ll R \ll \hbar c/\mathcal{L}$, and for very large separations $R \sim \hbar c/\mathcal{L}$. While a parametric analysis [Eq. (10)] would suggest dominance of the pole term in the intermediate range, a numerical calculation reveals a different behavior, with the Wick-rotated term dominating the interaction, due to the variability of the numerical coefficients multiplying the parametric estimates given in Eq. (10).

Conclusions.—We have shown that the consistent use of Feynman propagators and the concomitant virtual photon integration contours lead to the prediction of long-range tails for excited-state van der Waals interactions. Pole terms are picked up for virtual states $|v_A\rangle = |m_A\rangle$ of lower energy

than the reference state of the excited atom A . The pole contribution \mathcal{Q} to the energy shift is complex rather than real (includes a width term $\Gamma = -2\text{Im}\mathcal{Q}$), is space-wise oscillating and in the long range, behaves as $\cos[2(E_m - E_A)R/(\hbar c)]/R^2$, where E_A is the reference state energy and $E_m < E_A$ that of the low-energy virtual state. For excited states, both the direct as well as the exchange (gerade-ungerade mixing) term can be expressed as a sum of a Wick-rotated contribution [Eq. (4)], and a pole term [Eq. (5)]. Our inclusion of the nonresonant terms in the interaction energy enables us to match the very-long-range, oscillatory result against the well-known close-range, nonretarded van der Waals limit, and to carry out numerical calculations in the intermediate region. We also include the width term and the gerade-ungerade mixing term that pertains to excited-state interactions of identical atoms.

For $nD-1S$ interactions, we have shown that despite parametric suppression, the Wick-rotated term, which is nonoscillatory and contains the nonresonant states, still dominates in the intermediate distance range $a_0/\alpha \lesssim R \ll \hbar c/\mathcal{L}$ (see Fig. 2). The very-long-range, oscillatory tail of the van der Waals interaction is relevant only for very large interatomic distances. This conclusion holds for $nD-1S$ interactions as well as $nS-1S$ systems [19,23]. The reason for the suppression is that the numerical coefficients which multiply the parametric estimates given in Eq. (10) drastically depend on the particular term in the van der Waals energy. This is in part due to the scaling of the coefficients with the principal quantum number. For example, for $nD-1S$ interactions, the $1/R^2$ leading oscillatory tail from Eq. (5) is of order $E_h\alpha^4 \cos(\alpha\rho)/\rho^2$, yet multiplied by numerical coefficients of order 10^{-6} [in addition to the factor α^4 ; see the Supplemental Material [19], Eq. (14), Table I and Fig. 2]. By contrast, the nonoscillatory terms of order E_h/ρ^6 are multiplied by coefficients of order $10^4 \dots 10^6$. This behavior of the coefficients changes any predictions based on the parametric estimates given in Eq. (10) by 10 orders of magnitude as compared to a situation with coefficients of order unity.

Our results are important for an improved analysis of pressure shifts, and fluctuating-dipole-induced energy shift, for atomic beam spectroscopy with Rydberg states, where these effects have been identified as notoriously problematic in recent years (see pages 134 and 151 of Ref. [17]). An improved determination of the Rydberg constant based on Rydberg-state spectroscopy could resolve the muonic hydrogen proton radius puzzle, because the smaller proton radius measured in Refs. [24,25] leads to a Rydberg constant which is discrepant with regard to the current CODATA value [24,26].

This research has been supported by the NSF (Grant No. PHY-1403937).

- [1] H. B. G. Casimir and D. Polder, The Influence of Radiation on the London-van-der-Waals Forces, *Phys. Rev.* **73**, 360 (1948).
- [2] M. I. Chibisov, Dispersion interaction of neutral atoms, *Opt. Spectrosc.* **32**, 1 (1972).
- [3] W. J. Deal and R. H. Young, Long-range dispersion interactions involving excited atoms; the H(1s)—H(2s) interaction, *Int. J. Quantum Chem.* **7**, 877 (1973).
- [4] C. M. Adhikari, V. Debierre, A. Matveev, N. Kolachevsky, and U. D. Jentschura, Long-range interactions of hydrogen atoms in excited states. I. $2S-1S$ interactions and Dirac- δ perturbations, *Phys. Rev. A* **95**, 022703 (2017).
- [5] U. D. Jentschura, V. Debierre, C. M. Adhikari, A. Matveev, and N. Kolachevsky, Long-range interactions of excited hydrogen atoms. II. Hyperfine-resolved $2S-2S$ system, *Phys. Rev. A* **95**, 022704 (2017).
- [6] E. A. Power and T. Thirunamachandran, Dispersion forces between molecules with one or both molecules excited, *Phys. Rev. A* **51**, 3660 (1995).
- [7] H. Safari, S. Y. Buhmann, D.-G. Welsch, and H. T. Dung, Body-assisted van der Waals interaction between two atoms, *Phys. Rev. A* **74**, 042101 (2006).
- [8] H. Safari and M. R. Karimpour, Body-Assisted van der Waals Interaction between Excited Atoms, *Phys. Rev. Lett.* **114**, 013201 (2015).
- [9] P. R. Berman, Interaction energy of nonidentical atoms, *Phys. Rev. A* **91**, 042127 (2015).
- [10] P. W. Milonni and S. M. H. Rafsanjani, Distance dependence of two-atom dipole interactions with one atom in an excited state, *Phys. Rev. A* **92**, 062711 (2015).
- [11] M. Donaire, R. Gu erout, and A. Lambrecht, Quasiresonant van der Waals Interaction between Nonidentical Atoms, *Phys. Rev. Lett.* **115**, 033201 (2015).
- [12] M. Donaire, Two-atom interaction energies with one atom in an excited state: van der Waals potentials versus level shifts, *Phys. Rev. A* **93**, 052706 (2016).
- [13] L. Gomberoff, R. R. McLone, and E. A. Power, Long-Range Retarded Potentials between Molecules, *J. Chem. Phys.* **44**, 4148 (1966).
- [14] F. Biraben, J.-C. Garreau, L. Julien, and M. Allegrini, New Measurement of the Rydberg Constant by Two-Photon Spectroscopy of Hydrogen Rydberg States, *Phys. Rev. Lett.* **62**, 621 (1989).
- [15] B. de Beauvoir, F. Nez, L. Julien, B. Cagnac, F. Biraben, D. Touahri, L. Hilico, O. Acef, A. Clairon, and J. J. Zondy, Absolute Frequency Measurement of the $2S-8S/D$ Transitions in Hydrogen and Deuterium: New Determination of the Rydberg Constant, *Phys. Rev. Lett.* **78**, 440 (1997).
- [16] C. Schwob, L. Jozefowski, B. de Beauvoir, L. Hilico, F. Nez, L. Julien, F. Biraben, O. Acef, J. J. Zondy, and A. Clairon, Optical Frequency Measurement of the $2S-12D$ Transitions in Hydrogen and Deuterium: Rydberg Constant and Lamb Shift Determinations, *Phys. Rev. Lett.* **82**, 4960 (1999); Erratum, *Phys. Rev. Lett.* **86**, 4193(E) (2001).
- [17] J. C. deVries, Ph.D. thesis, Massachusetts Institute of Technology, Cambridge, MA, 2002, <https://dspace.mit.edu/handle/1721.1/4108>.
- [18] V. B. Berestetskii, E. M. Lifshitz, and L. P. Pitaevskii, *Quantum Electrodynamics, Volume 4 of the Course on*

- Theoretical Physics*, 2nd ed. (Pergamon Press, Oxford, UK, 1982).
- [19] See Supplemental Material at <http://link.aps.org/supplemental/10.1103/PhysRevLett.118.123001> which contains additional details on the matching procedure for the effective Hamiltonian, and on the numerical calculations for $nD-1S$ interactions.
- [20] H. A. Bethe, The Electromagnetic Shift of Energy Levels, *Phys. Rev.* **72**, 339 (1947).
- [21] R. Barbieri and J. Sucher, General Theory of Radiative Corrections to Atomic Decay Rates, *Nucl. Phys.* **B134**, 155 (1978).
- [22] H. A. Bethe and E. E. Salpeter, *Quantum Mechanics of One- and Two-Electron Atoms* (Springer, Berlin, 1957).
- [23] C. M. Adhikari *et al.* (to be published).
- [24] R. Pohl *et al.* (CREMA Collaboration), The size of the proton, *Nature (London)* **466**, 213 (2010).
- [25] R. Pohl *et al.* (CREMA Collaboration), Laser spectroscopy of muonic deuterium, *Science* **353**, 669 (2016).
- [26] P.J. Mohr, D.B. Newell, and B.N. Taylor, CODATA Recommended values of the fundamental physical constants: 2014, *Rev. Mod. Phys.* **88**, 035009 (2016).